PROCEEDINGS OF SCIENCE

Recent applications of the Simple Effective Interaction: The N=50 and Z=28 shell closure and charge radii differences of mirror nuclei

PoS(QNP2024)227

X. Viñas,[a,b,c,*] **P. Bano,**[d] **S.P. Pattnaik,**[d] **M. Centelles**[a,b] **and T.R. Routray**[d]

[a] *Departament de Física Quàntica i Astrofísica (FQA), Universitat de Barcelona (UB), Martí i Franquès 1, E-08028 Barcelona, Spain*

[b] *Institut de Ciències del Cosmos (ICCUB), Universitat de Barcelona (UB), Martí i Franquès 1, E-08028 Barcelona, Spain*

[c] *Institut Menorquí d'Estudis, Camí des Castell 28, 07702 Maó, Spain*

[d] *School of Physics, Sambalpur University, Jyotivihar 768019, India*

E-mail: xavier@fqa.ub.edu

We review the recent application of the so-called finite range simple effective interaction (SEI) to study the Ni and Cu isotopes with neutron number $N = 40$ to $N = 50$. Recent experiments performed in neutron-rich Cu isotopes have revealed a crossing between the $3/2^-$ and $5/2^-$ spin-parity of the ground state and first excited state in ^{75}Cu. In contrast to the common situation with Skyrme and other effective forces, where a tensor interaction needs to be added to account for this crossing and for the crossing of the $2p_{3/2}$ and $1f_{5/2}$ proton single-particle levels in Ni isotopes, we find that SEI is able to reproduce the experimental crossing without the necessity of adding a tensor interaction. We also study with SEI the correlation of the charge radii differences in mirror nuclei pairs with the neutron skin thickness and with the slope L of the symmetry energy. By comparing the SEI predictions with the measured charge radii difference in four mirror pairs and with the NICER astrophysical constraint for the radius of $1.4\,\mathrm{M}_\odot$ neutron stars, we obtain the constraint $L \approx$ 70–100 MeV. This range for L is discussed in the light of the recent PREX-2 and CREX data on the neutron skin thickness.

10th International Conference on Quarks and Nuclear Physics (QNP2024)
8-12 July, 2024
Barcelona, Spain

*Speaker

1. Introduction

The Simple Effective Interaction (SEI) was proposed by B. Behera and collaborators about twenty-five years ago [1] aimed to describe symmetric and asymmetric nuclear matter properties considering the trends of the results from microscopic Brueckner-Hartree-Fock (BHF) and Dirac-Brueckner-Hartree-Fock (DBHF) calculations. The SEI interaction consists of a finite-range term of Gauss or Yukawa type supplemented by two zero-range terms, one of them is a density-dependent term that simulates three-body contributions, plus a zero-range spin-orbit contribution to deal with finite nuclei:

$$\begin{aligned} V_{\text{eff}} &= t_0(1+x_0P_\sigma)\delta(\vec{r}) + \frac{t_3}{6}(1+x_3P_\sigma)\left(\frac{\rho(\vec{R})}{1+b\rho(\vec{R})}\right)^\gamma \delta(\vec{r}) \\ &+ (W+BP_\sigma - HP_\tau - MP_\sigma P_\tau)f(r/\alpha) + \text{Spin-orbit part}, \end{aligned} \tag{1}$$

where $f(r/\alpha)$ is the Gauss or Yukawa form factor. The SEI in Eq. (1) has 12 parameters in total, namely, $\alpha, \gamma, b, x_0, x_3, t_0, t_3, W, B, H,$ and M plus the spin-orbit strength parameter W_0, which enters in the description of finite nuclei. Ten of the twelve parameters of SEI have been fitted to symmetric and asymmetric nuclear matter properties, including constraints from the results predicted by BHF and DBHF calculations. The empirical condition that the nuclear mean field in symmetric nuclear matter at saturation density vanishes for the kinetic energy of the incident nucleon of 300 MeV is also imposed. A detailed description of the fitting protocol of the free parameters of SEI can be found in Ref. [2].

SEI has been applied in former studies of nuclear and neutron matter at zero and finite temperature and also in the astrophysical domain (see [2] and references therein). SEI has also been used in calculations of spherical [3–6] and deformed [7] finite nuclei. The finite nuclei calculation is performed using the Quasilocal Density Functional theory, explained in detail in [3] and references therein, which allows to write the non-local exchange energy in a local form with the help of the semiclassical Extended Thomas-Fermi density matrix.

Our aim in this contribution is to review our study [4, 6] of two recent problems of nuclear structure using SEI. One of them [4] concerns recent experiments performed in neutron-rich copper isotopes that have revealed the crossing between the $3/2^-$ and $5/2^-$ spin-parity of the ground state and first excited state in the nucleus ^{75}Cu [8]. Due to the strong single-particle character of these states, this problem can be investigated by means of the analysis of the proton spectrum provided by mean field models in nickel isotopes with neutron numbers between N=40 and N=50, in such a way that the spin-parity inversion in ^{75}Cu corresponds to the crossing between the $2p_{3/2}$ and $1f_{5/2}$ proton single-particle levels in ^{74}Ni. In order to reproduce this feature using mean-field models, it has been claimed that the use of a tensor contribution in the effective interaction is necessary, at least for Skyrme forces [9, 10]. In this contribution we will show that the mentioned crossing in nickel and copper isotopes can be explained satisfactorily by SEI without including any tensor contribution.

Another recent interesting problem that we have investigated with SEI [6] and that we will discuss here concerns the correlation between charge radii differences in mirror nuclei, ΔR_{CH}, and the neutron skin thickness, ΔR_{np}, which in turn can be related to the slope

Figure 1: (a) Proton single-particle energies around the Fermi level for Ni isotopes from A=68 to A=78 computed with the Skyrme forces SAMi-T and SLy5. (b) The same computed with SEI.

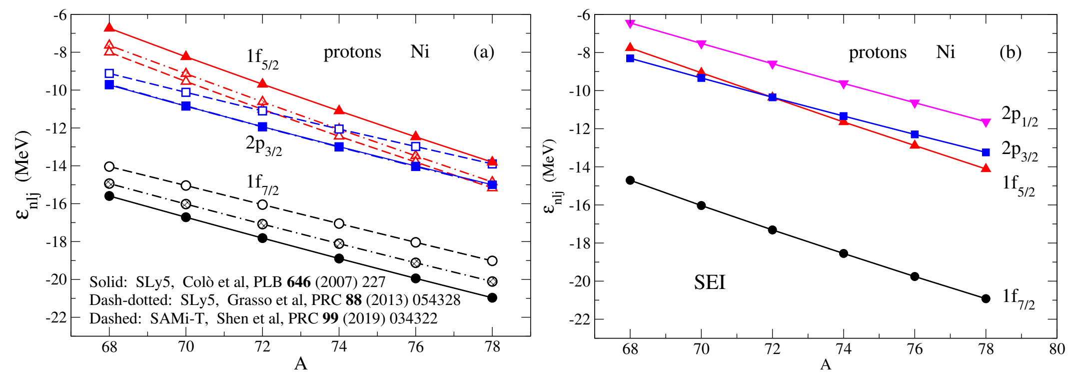

of the symmetry energy L [11]. The precisely measured ΔR_{CH} in the ^{34}Ar-^{34}S, ^{36}Ca-^{36}S, ^{38}Ca-^{38}S and ^{54}Ni-^{54}Fe mirror pairs allows us to estimate, using SEI, that the L value lies in the range $\approx$ 70–100 MeV. The SEI model in this range of L values explains the PREX-2 data for the neutron skin thickness of ^{208}Pb up to $\approx$ 30% of the experimental range. However, in the case of CREX experiment, only the lowest limit L=70 MeV is consistent with the upper limit of the neutron skin thickness in ^{48}Ca, 0.17 fm, predicted by CREX. On the basis of the correlation found between ΔR_{CH} in the ^{54}Ni-^{54}Fe mirror pair and ΔR_{np}, the SEI model predictions in the range L=70–100 MeV are consistent with the constraint of the radius of a neutron star of 1.4 $M_{\odot}$ mass, $R_{1.4} = 12.45 \pm 0.65$ km, extracted from the NICER data analysis for the pulsar PSR J0740+6620.

2. The N=50 and Z=28 shell closure

The left panel of Figure 1 shows the proton single-particle levels around the Fermi level for Ni isotopes from A=68 to A=78 computed with the Skyrme forces SAMi-T and SLy5 both including a tensor term. We can see that the force SAMi-T (dashed lines) predicts the crossing between the $2p_{3/2}$ and $1f_{5/2}$ single-particle levels while SLy5 with two different tensor contributions (solid lines and dash-dotted lines) is unable to predict this crossing. This fact points out that a tensor term in Skyrme forces is needed to reproduce the crossing of the $2p_{3/2}$ and $1f_{5/2}$ levels in neutron-rich Ni isotopes but, however, this condition may not be enough in some Skyrme forces. Something similar happens [4] with finite-range effective forces such as D1MT, which can reproduce the crossing only if an additional tensor term is included. However, as can be seen in the right panel of Figure 1, SEI is able to reproduce the crossing without including tensor terms. As discussed in Ref. [4], the behaviour of the single-particle levels predicted by different interactions is ruled by the monopole contributions of the central and spin-orbit parts of the interaction, which can be enough or not to reproduce the crossing of the $2p_{3/2}$ and $1f_{5/2}$ levels. As we have seen, the addition of a tensor term may help to reproduce the crossing.

Table 1: Spin-parity and energy of the ground-state and energy of the first excited state (E^*) of odd Cu isotopes predicted by the SEI model. The experimental energies (K.T. Flanagan et al, Phys. Rev. Lett. **103**, 14250 (2009)) are also reported.

Nucleus	Spin-Parity	Energy(SEI) (MeV)	Energy(exp) (MeV)	E^*(SEI) (keV)	E^*(exp) (keV)
^{69}Cu	$3/2^-$	-598.59	-599.97	794	1215
^{71}Cu	$3/2^-$	-612.93	-613.09	544	537
^{73}Cu	$3/2^-$	-625.76	-625.51	282	263
^{75}Cu	$3/2^-$	-637.49	-637.13	72	62
^{77}Cu	$5/2^-$	-648.38	-647.42	246	295
^{79}Cu	$5/2^-$	-658.19	-656.65	525	660

Figure 2: Neutron skin thickness as a function of the proton radii difference in mirror pairs.

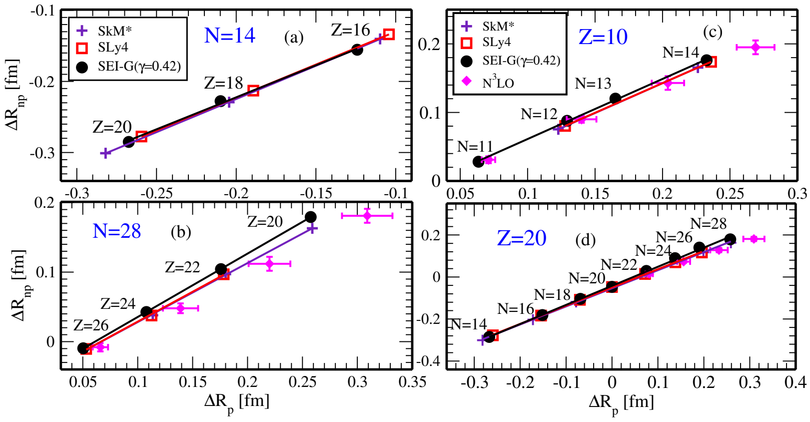

In Table 1 we display the ground-state spin-parity and the energy of the ground state of neutron-rich odd Cu isotopes predicted by the SEI model used in this work. The energy of the first excited state E^* predicted by SEI is reported in the same table, together with the experimental data. Noticeably, according to the SEI calculations the crossing between the $3/2^-$ and $5/2^-$ occurs for ^{75}Cu and the first excited state lies 72 keV above the ground state, in good agreement with the experimental data.

3. Charge radii differences of mirror nuclei, symmetry energy and neutron star radii

Under strict isospin symmetry the neutron skin thickness in a nucleus becomes the proton radius difference in a pair of mirror nuclei: $\Delta R_p = R_p(N,Z) - R_p(Z,N)$. When Coulomb and other symmetry breaking effects are taken into account, ΔR_{np} and ΔR_p in the mirror pair are still correlated, as can be seen in Figure 2, where ΔR_{np} is plotted as a function of ΔR_p computed with SEI ($\gamma = 0.42$) for the isotonic chains of (a) N=14

PoS(QNP2024)227

Figure 3: (a)-(d): Charge radii differences for mirror pairs against the slope of the symmetry energy. (e)-(h): Neutron skin thickness of selected nuclei against the slope of the symmetry energy.

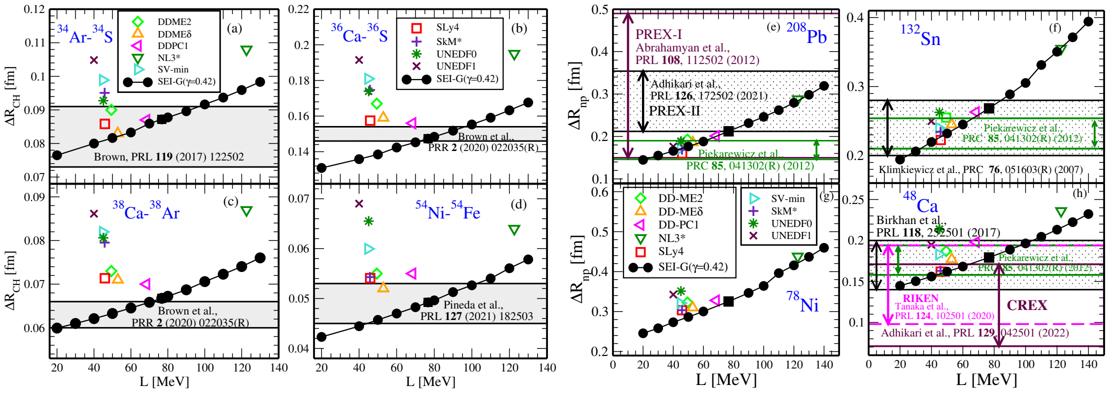

and (b) N=28, and for the isotopic chains of (c) Z=10 and (d) Z=2. We also show the results obtained with SkM*, SLy4 and N^{3}LO forces. Using the SEI data, we find the linear correlation $\Delta R_{np} = (0.881 \pm 0.036)\,\Delta R_p + (-0.049 \pm 0.017)$ fm, between the neutron skin and the proton radii difference. The SEI model with the characteristic slope of the symmetry energy L_c=76.71 MeV [6] reproduces very nicely the four $\Delta R_{\rm CH}$ values of mirror pairs for which experimental information is available: ^{34}Ar-^{34}S 0.087 (exp: 0.082(9)) fm, ^{36}Ca-^{36}S 0.147 (exp: 0.150(4)) fm, ^{38}Ca-^{38}Ar 0.066 (exp: 0.063(3)) fm, and ^{54}Ni-^{54}Fe 0.049 (exp: 0.049(4)) fm, where the experimental data are between round brackets.

Since long ago [11] it is known that the neutron skin thickness in a heavy nucleus is linearly correlated with L. On the other hand, the SEI model is flexible enough to allow imposing in the fitting procedure a value of the slope of the symmetry energy L different from the characteristic one L_c in such a way that the binding energies and radii of finite nuclei are practically unaffected by the change in L (see [6] for more details). Taking into account these facts and the ΔR_p–ΔR_{np} correlation discussed previously (see Figure 2), we plot in the panels (a)-(d) of Figure 3 the charge radii difference in mirror pairs as a function of L, which show a nice linear correlation as expected. In the same figure we also display the bands corresponding to the experimental values of the charge radii difference including their error bars. This allows us to estimate that L lies in the range 70–100 MeV. The slope of the symmetry energy can also be estimated from other experiments, as for instance the elastic scattering of polarized electrons (PREX and CREX experiments) or pygmy resonance studies. In panels (e)-(h) of Figure 3 we display the neutron skin thickness as a function of the slope of the symmetry energy for the nuclei ^{208}Pb, ^{132}Sn, ^{78}Ni and ^{48}Ca predicted by SEI. From this figure we see that the lower bound of the neutron skin in ^{208}Pb predicted by PREX-2 can be reached by SEI with the L_c value, but the PREX-2 central value, 0.283 fm, requires to use L=122 MeV in the SEI model. The recently measured neutron skin thickness ^{48}Ca in CREX, $\Delta R_{np} = 0.121 \pm 0.05$ fm, implies that SEI predictions can still remain within the CREX uncertainty limit if $L \leq 65$ MeV is used, but to recover the CREX central value, 0.121 fm, demands a L value below the lowest limit of 20 MeV, extracted from the charge radii difference-L correlation.

The correlation between the neutron skin thickness in ^{208}Pb and the radius of neutron stars was investigated long ago [12, 13]. Due to the fact that within the SEI model ΔR_{np} in ^{208}Pb is strongly correlated with the charge radii difference $\Delta R^{54}_{\rm CH}$ in the ^{54}Ni-^{54}Fe pair, it is appealing to study the correlation between $\Delta R^{54}_{\rm CH}$ and the radius of neutron stars. We find a good linear correlation between these two quantities for neutron star masses ranging from 0.8 $M_\odot$ to 1.8 $M_\odot$, see Ref. [6]. The NICER data analysis of the signals from the pulsar PSR J0740+6620 predicts a radius $R_{1.4} = 12.45 \pm 0.65$ km for the 1.4 $M_\odot$ neutron star, which is compatible with the value $R_{1.4} = 13.9 \pm 1.4$ km extracted from the data analysis of the GW170817 event. Combining the $R_{1.4}$-$\Delta R^{54}_{\rm CH}$ and L-$\Delta R_{\rm CH}$ correlations (see left panel of Figure 3), we find that the observed radius of the 1.4 $M_\odot$ neutron star constrains the slope of the symmetry energy predicted by SEI to the range $\approx$ 70–100 MeV, which is consistent with our estimate based on the charge radii difference in mirror nuclei and compatible with the values of L extracted from the analysis of other different experimental data (see [6] for further details). Finally, we point out that in this range of L values, the tidal deformability $\Lambda_{1.4} = 190^{+390}_{-120}$ extracted from the GW170817 event is well reproduced by the SEI predictions [6].

References

[1] B. Behera, T.R. Routray and R.K. Satpathy, J. Phys. G **24** (1998) 2073.

[2] X. Viñas, P. Bano, Z. Naik and T.R. Routray, Symmetry **16** (2024) 215.

[3] B. Behera, X. Viñas et al., J. Phys. G **40** (2013) 095105.

[4] T.R. Routray, P. Bano et al., Phys. Rev. C **104** (2021) L011302.

[5] P. Bano, X. Viñas, T.R. Routray, M. Centelles, M. Anguiano, and L.M. Robledo, Phys. Rev. C **106** (2022) 024313.

[6] P. Bano, S.P. Pattnaik, M. Centelles, X. Viñas and T. R. Routray, Phys. Rev. C **108** (2023) 015802.

[7] B. Behera, X. Viñas et al., J. Phys. G **43** (2016) 045115.

[8] I. Stefanescu, G. Georgiev, D.L. Balabanski et al., Phys. Rev. Lett. **100** (2008) 112502.

[9] F. Stancu, D.M. Brink, and H. Flocard, Phys. Lett. B **68** (1977) 108.

[10] D.M. Brink and F. Stancu, Phys. Rev. C **97** (2018) 064304.

[11] B.A. Brown, Phys. Rev. Lett. **85** (2000) 5296.

[12] C.J. Horowitz and J. Piekarewicz, Phys. Rev. C **64** (2001) 062802(R).

[13] J. Carriere, C.J. Horowitz and J. Piekarewicz, Astrophys. J. **593** (2003) 463.